Smart Structures and Systems, *Vol. 16, No. 5 (2015) 853-872*
DOI: http://dx.doi.org/10.12989/sss.2015.16.5.853

Large amplitude free vibration analysis of laminated composite spherical shells embedded with piezoelectric layers

Vijay K. Singh[a] and Subrata K. Panda[*]

Department of Mechanical Engineering, National Institute of Technology, Rourkela-769008, Odisha, India

(Received February 6, 2015, Revised May 1, 2015, Accepted May 2, 2015)

Abstract. Numerical analysis of large amplitude free vibration behaviour of laminated composite spherical shell panel embedded with the piezoelectric layer is presented in this article. For the investigation purpose, a general nonlinear mathematical model has been developed using higher order shear deformation mid-plane kinematics and Green-Lagrange nonlinearity. In addition, all the nonlinear higher order terms are included in the present mathematical model to achieve any general case. The nonlinear governing equation of freely vibrated shell panel is obtained using Hamilton's principle and discretised using isoparametric finite element steps. The desired nonlinear solutions are computed numerically through a direct iterative method. The validity of present nonlinear model has been checked by comparing the responses to those available published literature. In order to examine the efficacy and applicability of the present developed model, few numerical examples are solved for different geometrical parameters (fibre orientation, thickness ratio, aspect ratio, curvature ratio, support conditions and amplitude ratio) with and/or without piezo embedded layers and discussed in details.

Keywords: nonlinear vibration; laminated composites; Green-Lagrange nonlinearity; PZT; HSDT; nonlinear finite element method; spherical shell panel

1. Introduction

Smart structures have got huge attention over the last two decades due to their coupling between electric, magnetic, thermal and/or mechanical effects for achieving the desired performance in modern structural systems. This lead to wide area of applications in structural health monitoring, vibration isolation and/or control, shape control, medical applications, damage detection and noise attenuation. Smart materials are also well known for their physical coupling effect which make them useful as sensors and/or actuators in different high-performance engineering structures. Out of all the available smart materials, piezoelectric materials remain the most widely used due to their advantages like higher structural stiffness/strength and voltage dependent actuation. Moreover, these materials are less expensive, light in weight, commercially available in different shapes and can be bonded easily to any other surfaces of material using commonly available adhesives. It is well known that the coupling of mechanical and electrical

*Corresponding author, Assistant Professor, E-mail: call2subrat@gmail.com
[a] Research scholar, E-mail: vijaynitr12@gmail.com

http://www.techno-press.org/?journal=sss&subpage=8 ISSN: 1738-1584 (Print), 1738-1991 (Online)

properties are governed by converse and direct piezoelectric effect which in turn make them well suited for sensors and/or actuators. The piezoelectric materials are used in the form of layers/patches embedded and/or surface bonded to the parent structure/structural components. Based on the advantages, piezoelectric ceramic materials (lead zirconate titanate, PZT) have been chosen as the smart material for this present investigation.

Many researches have already been completed on the modelling of laminated composite plate/shell structures embedded and/or surface bonded piezoelectric layers using analytical and numerical methods. Arefi and Khoshgoftar (2014) developed coupled piezo-thermo-elastic generalized model of thick functionally graded hollow spherical shell panel embedded with piezoelectric material under electro-thermo-mechanical loads to improve the relation between mechanical and electrical load. Arefi and Rahimi (2011) investigated nonlinear responses of functionally graded (FG) square plate bonded with two smart layers acting as sensor and actuator under uniform pressure by considering the nonlinearity in von-Karman sense. Benjeddou (2000) presented exhaustive review on advances and trends in finite element method for the analysis of adaptive structures. Balamurugan and Narayanan (2001, 2009) investigated active vibration control performance of piezo bonded laminated flat and shell structures by taking the coupled (mechanical and electrical) load effect and solved using finite element method (FEM). They have modelled the electric potential through a higher order approximation. Benjeddou *et al*. (2002) reported exact two-dimensional analytical solutions for free vibration behaviour of piezoelectric bonded adaptive plate using layerwise first order shear deformation theory (FSDT) and quadratic non-uniform electric potential. Chakravorty *et al.* (1996) investigated linear free vibration behaviour of thin shallow doubly curved shell panel by taking the effect of various geometrical and/or material properties using FSDT mid-plane kinematics. Das and Singh (2009) investigated nonlinear free vibration behaviour of laminated composite plate embedded with piezoelectric layers based on higher-order shear deformation theory (HSDT) and Green-Lagrange nonlinearity. Heyliger and Brooks (1995) reported free vibration responses of piezoelectric laminated plates with cylindrical bending and also computed the natural frequencies through thickness modal distributions of elastic and electric field variables. Huang and Shen (2005) presented nonlinear free vibration and dynamic behaviour of laminated plates embedded with piezoelectric actuators under the action of mechanical, electrical and thermal loads. Huang and Sun (2001) investigated dynamic responses of the composite beam bonded with piezoelectric sensors and actuators. Kattimani and Ray (2014) examined large amplitude vibration suppression of doubly curved shell panel using active constrained layer damping (ACLD) effect under magneto-electro-elastic (MEE) load. Lee and Reddy (2004) reported analytical solutions of vibration suppression of laminated composite shells with smart material layers using von-Karman nonlinearity in the framework of Donnell and Sanders shell kinematic. Lee *et al.* (2006) investigated the degree of deflection suppression of laminated composite shells bonded with smart layer through nonlinear finite element (FE) steps. The model has been developed using Sanders nonlinear shell kinematics in the framework of HSDT. Nanda (2010) investigated the effects of voltage and different geometrical parameters on the nonlinear free vibration and transient responses of composite shell panels bonded with piezoelectric layers under uniform thermal environment. Kerur and Ghosh (2011) reported the active control of nonlinear transient responses of laminated composite plate using the FSDT kinematics and von-Karman nonlinearity under coupled electromechanical loading. Rafiee *et al.* (2013) studied nonlinear free vibration and dynamic behaviour of piezoelectric bonded FG shells under combined electrical, thermal, mechanical and aerodynamic loading. Ramirez *et al.* (2006) presented free vibration responses of two-dimensional MEE laminates using discrete layer

approach through Ritz method. Reddy (1999) reported Navier's solutions of smart laminated composite plate under mechanical and electrical loading. The plate model has been developed using classical and shear deformation theories and discretised using FE steps. Saravanos *et al.* (1997) presented dynamics behaviour composite plate embedded with piezoelectric actuators and sensors using layerwise theory. Geometrical nonlinear transient response of doubly curved shell panel and laminated composite beam embedded in 1-3 piezoelectric composite material are computed using FSDT kinematics and von-Karman nonlinearity by Sarangi and Ray (2010, 2011). Singh and Panda (2014) developed a geometrical nonlinear mathematical model to analyse large amplitude free vibration behaviour of doubly curved composite shell panel using HSDT kinematics and Green Lagrange type nonlinearity. Xu *et al.* (1997) presented analytical 3D solution of free vibration responses of cross-ply hybrid composite plates by considering the effect of piezo-thermo-elastic layers. Kulkarni and Bajoria (2007) investigated geometrically nonlinear behaviour of piezo laminated smart composite plates and shells by taking von-Karman nonlinearity in the framework of HSDT and FSDT mid-plane kinematics.

It is clear from the above review that no study has been reported yet in open literature on the nonlinear free vibration behaviour of laminated composite spherical shell panel bonded with piezoelectric layers based on the HSDT mid-plane kinematics and Green-Lagrange nonlinearity. Hence the present study aims to develop a nonlinear mathematical model of laminated composite spherical shell panel embedded with PZT layer for the closed-circuit configuration (external surfaces are grounded i.e., electric potential 'ϕ' zero at the top and bottom surfaces) to analyse the large amplitude free vibration responses. The model has been developed based on the HSDT kinematics and Green-Lagrange nonlinearity by including all the nonlinear higher order terms to achieve the generality. The nonlinear governing equation is obtained using Hamilton's principle and discretised through isoparametric finite element steps. The desired nonlinear responses are computed by solving the governing equations numerically through a direct iterative method. The validity and competency of the developed model have been established by comparing the responses to those available published literature. The applicability of the proposed model has been shown by solving wide variety of examples for different parameters such as stacking sequences, thickness ratios, amplitude ratios, curvature ratios, support conditions, symmetric and unsymmetrical laminations and aspect ratios and discussed in details.

2. Mathematical formulations

In this analysis, a doubly curved laminated composite shallow shell of uniform thickness 'h' is considered (Fig. 1). For the present study, it is assumed that the piezoelectric actuators are bonded to the outermost surfaces of the laminated shell panel and are poled in the thickness direction. The principal radii of curvatures of shallow shell panel are, R_x and R_y (twist radius of curvature $R_{xy} = \infty$) along x and y directions, respectively. The projection of shell on the xy-plane is a rectangle of dimensions 'a' and 'b' (Fig. 1).

2.1 Element geometry and displacement field

The displacement field within the laminate is assumed to be based on the HSDT (Reddy 2004) kinematics. This field represents that, the in-plane displacements are expanded as cubic functions of thickness coordinate while the transverse displacement varies linearly through the laminate

thickness

$$\begin{aligned} u^{(k)}(x,y,z,t) &= u_0(x,y) + z\theta_x(x,y) + z^2\phi_x(x,y) + z^3\lambda_x(x,y) \\ v^{(k)}(x,y,z,t) &= v_0(x,y) + z\theta_y(x,y) + z^2\phi_y(x,y) + z^3\lambda_y(x,y) \\ w^{(k)}(x,y,z,t) &= w_0(x,y) + z\theta_z(x,y) \end{aligned} \tag{1}$$

where, $u^{(k)}$, $v^{(k)}$ and $w^{(k)}$ denote the displacements of a point along the (x, y, and z) coordinates in the k^{th} layer in function of corresponding mid-plane displacements u_0, v_0 and w_0 at time t. θ_x and θ_y are the rotations of normal to the mid-surface i.e., z=0 about the y and x-axes, respectively. The functions $\phi_x, \phi_y, \lambda_x, \lambda_y$ and θ_z are the higher order terms in the Taylor series expansion.

2.2 Strain displacement relations

The nonlinear Green–Lagrange strain–displacement relation for the laminated doubly curved shell panel can be expressed as in Singh and Panda (2014).

$$\{\varepsilon\} = \begin{Bmatrix} \varepsilon_{xx} \\ \varepsilon_{yy} \\ \varepsilon_{zz} \\ \varepsilon_{yz} \\ \varepsilon_{xz} \\ \varepsilon_{xy} \end{Bmatrix} = \begin{Bmatrix} \left(\frac{\partial u}{\partial x} + \frac{w}{R_x}\right) \\ \left(\frac{\partial v}{\partial y} + \frac{w}{R_y}\right) \\ \left(\frac{\partial w}{\partial z}\right) \\ \left(\frac{\partial v}{\partial z} + \frac{\partial w}{\partial y} - \frac{v}{R_y}\right) \\ \left(\frac{\partial u}{\partial z} + \frac{\partial w}{\partial x} - \frac{u}{R_x}\right) \\ \left(\frac{\partial u}{\partial y} + \frac{\partial v}{\partial x} + \frac{2w}{R_{xy}}\right) \end{Bmatrix} + \frac{1}{2} \begin{Bmatrix} \left[\left(\frac{\partial u}{\partial x} + \frac{w}{R_x}\right)^2 + \left(\frac{\partial v}{\partial x} + \frac{w}{R_{xy}}\right)^2 + \left(\frac{\partial w}{\partial x} - \frac{u}{R_x}\right)^2\right] \\ \left[\left(\frac{\partial u}{\partial y} + \frac{w}{R_{xy}}\right)^2 + \left(\frac{\partial v}{\partial y} + \frac{w}{R_y}\right)^2 + \left(\frac{\partial w}{\partial y} - \frac{v}{R_y}\right)^2\right] \\ \left[\left(\frac{\partial u}{\partial z}\right)^2 + \left(\frac{\partial v}{\partial z}\right)^2 + \left(\frac{\partial w}{\partial z}\right)^2\right] \\ 2\left[\frac{\partial u}{\partial z}\left(\frac{\partial u}{\partial y} + \frac{w}{R_{xy}}\right) + \frac{\partial v}{\partial z}\left(\frac{\partial v}{\partial y} + \frac{w}{R_y}\right) + \frac{\partial w}{\partial z}\left(\frac{\partial w}{\partial y} - \frac{v}{R_y}\right)\right] \\ 2\left[\frac{\partial u}{\partial z}\left(\frac{\partial u}{\partial x} + \frac{w}{R_x}\right) + \frac{\partial v}{\partial z}\left(\frac{\partial v}{\partial x} + \frac{w}{R_{xy}}\right) + \frac{\partial w}{\partial z}\left(\frac{\partial w}{\partial x} - \frac{u}{R_x}\right)\right] \\ 2\left[\left(\frac{\partial u}{\partial y} + \frac{w}{R_{xy}}\right)\left(\frac{\partial u}{\partial x} + \frac{w}{R_x}\right) + \left(\frac{\partial v}{\partial y} + \frac{w}{R_y}\right)\left(\frac{\partial v}{\partial x} + \frac{w}{R_{xy}}\right) + \left(\frac{\partial w}{\partial y} - \frac{v}{R_y}\right)\left(\frac{\partial w}{\partial x} - \frac{u}{R_x}\right)\right] \end{Bmatrix} \tag{2a}$$

The total strain vector $\{\varepsilon\}$ is the summation of the linear $\{\varepsilon_L\}$ and nonlinear $\{\varepsilon_{NL}\}$ strain vector as follows

$$\{\varepsilon\} = \{\varepsilon_L\} + \{\varepsilon_{NL}\} \tag{2b}$$

Now, substituting Eq. (1) in Eq. (2(a)) the total strain can be expressed in terms of displacement and conceded as

$$\{\varepsilon_L\}+\{\varepsilon_{NL}\}=\begin{Bmatrix}\varepsilon_1^{l_0}\\ \varepsilon_2^{l_0}\\ \varepsilon_3^{l_0}\\ \varepsilon_4^{l_0}\\ \varepsilon_5^{l_0}\\ \varepsilon_6^{l_0}\end{Bmatrix}+\frac{1}{2}\begin{Bmatrix}\varepsilon_1^{nl_0}\\ \varepsilon_2^{nl_0}\\ \varepsilon_3^{nl_0}\\ 2\varepsilon_4^{nl_0}\\ 2\varepsilon_5^{nl_0}\\ 2\varepsilon_6^{nl_0}\end{Bmatrix}+z\left[\begin{Bmatrix}k_1^{l_1}\\ k_2^{l_1}\\ 0\\ k_4^{l_1}\\ k_5^{l_1}\\ k_6^{l_1}\end{Bmatrix}+\frac{1}{2}\begin{Bmatrix}k_1^{nl_1}\\ k_2^{nl_1}\\ k_3^{nl_1}\\ 2k_4^{nl_1}\\ 2k_5^{nl_1}\\ 2k_6^{nl_1}\end{Bmatrix}\right]+z^2\left[\begin{Bmatrix}k_1^{l_2}\\ k_2^{l_2}\\ 0\\ k_4^{l_2}\\ k_5^{l_2}\\ k_6^{l_2}\end{Bmatrix}+\frac{1}{2}\begin{Bmatrix}k_1^{nl_2}\\ k_2^{nl_2}\\ k_3^{nl_2}\\ 2k_4^{nl_2}\\ 2k_5^{nl_2}\\ 2k_6^{nl_2}\end{Bmatrix}\right]$$

$$+z^3\left[\begin{Bmatrix}k_1^{l_3}\\ k_2^{l_3}\\ 0\\ k_4^{l_3}\\ k_5^{l_3}\\ k_6^{l_3}\end{Bmatrix}+\frac{1}{2}\begin{Bmatrix}k_1^{nl_3}\\ k_2^{nl_3}\\ k_3^{nl_3}\\ 2k_4^{nl_3}\\ 2k_5^{nl_3}\\ 2k_6^{nl_3}\end{Bmatrix}\right]+z^4\frac{1}{2}\begin{Bmatrix}k_1^{nl_4}\\ k_2^{nl_4}\\ k_3^{nl_4}\\ k_4^{nl_4}\\ k_5^{nl_4}\\ k_6^{nl_4}\end{Bmatrix}+z^5\frac{1}{2}\begin{Bmatrix}k_1^{nl_5}\\ k_2^{nl_5}\\ k_3^{nl_5}\\ 2k_4^{nl_5}\\ 2k_5^{nl_5}\\ 2k_6^{nl_5}\end{Bmatrix}+z^6\frac{1}{2}\begin{Bmatrix}k_1^{nl_6}\\ k_2^{nl_6}\\ 0\\ 0\\ 0\\ 2k_6^{nl_6}\end{Bmatrix} \tag{3}$$

Now the above strain–displacement relation can be rearranged in matrix form as follows

$$\{\varepsilon_L\}+\{\varepsilon_{NL}\}=\left[T^L\right]\{\overline{\varepsilon_L}\}+\frac{1}{2}\left[T^{NL}\right]\{\overline{\varepsilon_{NL}}\} \tag{4a}$$

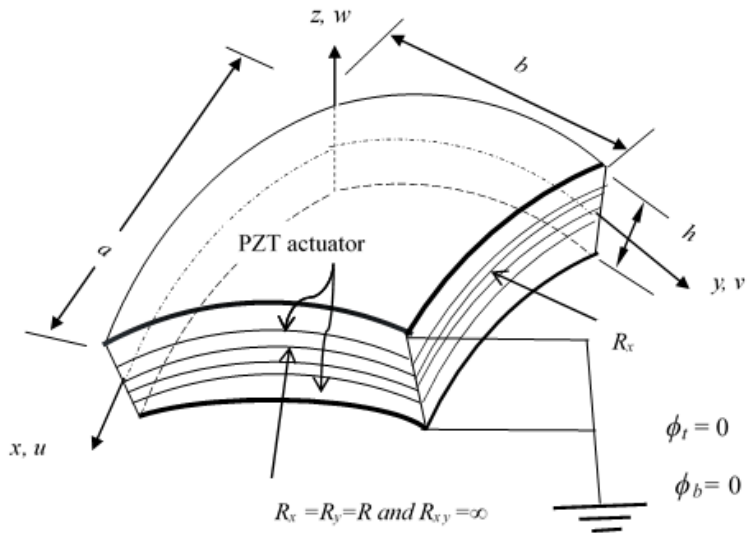

Fig. 1 Closed-circuit configuration of spherical laminated composite shell panel bonded with PZT layers

where, $\left\{\overline{\varepsilon_L}\right\}=\left\{\varepsilon_1^{l_0}\varepsilon_2^{l_0}\varepsilon_3^{l_0}\varepsilon_4^{l_0}\varepsilon_5^{l_0}\varepsilon_6^{l_0}k_1^{l_1}k_2^{l_1}k_4^{l_1}k_5^{l_1}k_6^{l_1}k_1^{l_2}k_2^{l_2}k_4^{l_2}k_5^{l_2}k_6^{l_2}k_1^{l_3}k_2^{l_3}k_4^{l_3}k_5^{l_3}k_6^{l_3}\right\}^T$ and $\begin{Bmatrix}\varepsilon_1^{nl_0} & \varepsilon_2^{nl_0} & \varepsilon_3^{nl_0} & \varepsilon_4^{nl_0} & \varepsilon_5^{nl_0} & \varepsilon_6^{nl_0} & k_1^{nl_1} & k_2^{nl_1} & k_3^{nl_1} & k_4^{nl_1} & k_5^{nl_1} & k_6^{nl_1} & k_1^{nl_2} & k_2^{nl_2} & k_3^{nl_2} & k_4^{nl_2} & k_5^{nl_2} & k_6^{nl_2} & k_1^{nl_3}\\ k_2^{nl_3} & k_3^{nl_3} & k_4^{nl_3} & k_5^{nl_3} & k_6^{nl_3} & k_1^{nl_4} & k_2^{nl_4} & k_3^{nl_4} & k_4^{nl_4} & k_5^{nl_4} & k_6^{nl_4} & k_1^{nl_5} & k_2^{nl_5} & k_4^{nl_5} & k_5^{nl_5} & k_6^{nl_5} & k_1^{nl_6} & k_2^{nl_6} & k_6^{nl_6}\end{Bmatrix}$ are the mid-plane linear and nonlinear strain terms. Similarly, $\left[T^L\right]$ and $\left[T^{NL}\right]$ are the function of thickness coordinate matrices for linear and nonlinear cases, respectively. The terms containing superscripts 'l_0', 'l_1', 'l_2-l_3'in $\left\{\overline{\varepsilon_L}\right\}$ and 'nl_0', 'nl_1', '$nl_{2—6}$'in $\left\{\overline{\varepsilon_{NL}}\right\}$ are the membrane, curvature and higher order strain terms, respectively.

The vectors $\left\{\overline{\varepsilon_L}\right\}$ and $\left\{\overline{\varepsilon_{NL}}\right\}$ can further be expressed as

$$\left\{\overline{\varepsilon_L}\right\}=\left[B_L\right]\{d\} \tag{4b}$$

$$\left\{\overline{\varepsilon_{NL}}\right\}=\tfrac{1}{2}\left[B_{NL}\right]\{d\} \tag{4c}$$

where, $\left[B_L\right]$and $\left[B_{NL}\right]$are linear and nonlinear operator matrices and $\{d\}$ is the displacement field vector and the individual terms can be seen in Singh and Panda (2014).

2.3 Piezoelectric constitutive relations

The transformed stress–strain relations for any general k^{th} orthotropic composite lamina embedded with the piezoelectric layer is conceded as follows

$$\{\sigma\}=\left[\overline{Q}\right]\{\varepsilon\}-\left[e\right]\{E\} \quad \text{and} \quad \left[D\right]=\left[e\right]^T\{\varepsilon\}+\left[\in\right]\{E\} \tag{5a}$$

The sensor and actuator equations may further be expanded as

$$\begin{Bmatrix}\sigma_1\\ \sigma_2\\ \sigma_3\\ \sigma_4\\ \sigma_5\\ \sigma_6\end{Bmatrix}^k=\begin{bmatrix}Q_{11} & Q_{12} & Q_{13} & 0 & 0 & 0\\ Q_{12} & Q_{22} & Q_{23} & 0 & 0 & 0\\ Q_{13} & Q_{23} & Q_{33} & 0 & 0 & 0\\ 0 & 0 & 0 & Q_{44} & 0 & 0\\ 0 & 0 & 0 & 0 & Q_{55} & 0\\ 0 & 0 & 0 & 0 & 0 & Q_{55}\end{bmatrix}^k\begin{Bmatrix}\varepsilon_1\\ \varepsilon_2\\ \varepsilon_3\\ \varepsilon_4\\ \varepsilon_5\\ \varepsilon_6\end{Bmatrix}^k-\begin{bmatrix}0 & 0 & e_{31}\\ 0 & 0 & e_{32}\\ 0 & 0 & e_{33}\\ 0 & e_{24} & 0\\ e_{15} & 0 & 0\\ 0 & 0 & 0\end{bmatrix}\begin{Bmatrix}E_1\\ E_2\\ E_3\end{Bmatrix} \tag{5b}$$

$$\begin{Bmatrix}D_1\\ D_2\\ D_3\end{Bmatrix}=\begin{bmatrix}0 & 0 & 0 & 0 & e_{15} & 0\\ 0 & 0 & 0 & e_{24} & 0 & 0\\ e_{31} & e_{32} & e_{33} & 0 & 0 & 0\end{bmatrix}\begin{Bmatrix}\varepsilon_1\\ \varepsilon_2\\ \varepsilon_3\\ \varepsilon_4\\ \varepsilon_5\\ \varepsilon_6\end{Bmatrix}+\begin{bmatrix}\in_{11} & 0 & 0\\ 0 & \in_{22} & 0\\ 0 & 0 & \in_{33}\end{bmatrix}\begin{Bmatrix}E_1\\ E_2\\ E_3\end{Bmatrix} \tag{5c}$$

where, $\{\sigma\}^k$,$\{\varepsilon\}^k$, $\left[Q\right]^k$,$\left[e\right]$,$\left[\in\right]$and $\left[E\right]$are stress tensor, strain tensor, transformed reduced

elastic constant matrix, piezoelectric constant matrix, dielectric constant matrix and electric field vectors, respectively for any orthotropic k^{th} layer.

$$\{E\}^T = \left\{ -\frac{\partial \phi}{\partial x} \quad -\frac{\partial \phi}{\partial x} \quad -\frac{\partial \phi}{\partial x} \right\}^T \tag{6}$$

Electric potential (ϕ) can be expressed as

$$\phi(x, y, z) = \phi^{(0)}(x, y) + z\phi^{(1)}(x, y) + z^2\phi^{(2)}(x, y) \tag{7}$$

The electric field vector $\{E\}$ can be expressed as

$$\{E\} = [T_\phi]\{E^0\} \tag{8}$$

where, $\{E^0\}^T = [B_\phi]\{\phi\} = \{E_x^{(0)} \quad E_y^{(0)} \quad E_x^{(1)} \quad E_y^{(1)} \quad E_x^{(2)} \quad E_y^{(2)} \quad X^{(1)} \quad X^{(2)}\}^T$ and $[B_\phi]$ and $[T_\phi]$ are the differential operator and thickness coordinate matrices correspond to potential field $\{\phi\}$, respectively. The details of the matrices are presented in Appendix A.

2.4 Total potential energy (U)

The total potential energy of PZT bonded laminated composite panel is obtained using the following steps

$$U = \frac{1}{2}\left(\int_V \{\varepsilon\}^T \{\sigma\}\, dV - \int_V \{E\}^T \{D\}\, dV \right) \tag{9a}$$

$$U = \frac{1}{2}\int_A \begin{pmatrix} \{\bar{\varepsilon}\}^T [D_1]\{\bar{\varepsilon}\} + \{\bar{\varepsilon}\}^T [D_4]\{\overline{\varepsilon_{nl}}\} \\ + \{\overline{\varepsilon_{nl}}\}^T [D_5]\{\bar{\varepsilon}\} + \{\overline{\varepsilon_{nl}}\}^T [D_6]\{\overline{\varepsilon_{nl}}\} \\ - \{\bar{\varepsilon}\}^T [D_2]\{E^0\} - \{\overline{\varepsilon_{nl}}\}^T [D_7]\{E^0\} \\ - \{E^0\}^T [D_2]\{\bar{\varepsilon}\} - \{E^0\}^T [D_8]\{\overline{\varepsilon_{nl}}\} - \{E^0\}^T [D_3]\{E^0\} \end{pmatrix} dA \tag{9b}$$

where, $[D_1]$, $[D_2]$, $[D_3]$, $[D_4]$, $[D_5]$, $[D_6][D_7]$and $[D_8]$ are the stiffnesses of the laminate with piezoelectric layers.

2.5 Kinetic energy (T)

The kinetic energy of the laminates is given by

$$T = \frac{1}{2}\iint \left[\sum_{k=1}^{N} \int_{h_k}^{h_{k+1}} \rho_k \left\{ \dot{u}_k \; \dot{v}_k \; \dot{w}_k \right\} \left\{ \dot{u}_k \; \dot{v}_k \; \dot{w}_k \right\}^T dz \right] dxdy \tag{10}$$

where, ρ_k is the mass density, h_k and h_{k+1} are the z coordinates of laminates corresponding to the top and bottom surface of the k^{th} layer and N is the number of laminae.

3. Finite element model

The developed nonlinear HSDT model is discretized using displacement finite element formulation steps. For the discretization purpose a nine-nodded isoparametric element with 10 degrees of freedom per node is used, namely u_0, v_0, w_0, θ_x, θ_y, θ_z, ϕ_x, ϕ_y, λ_x , λ_x. The displacement vector $\{de\}$, the electric potential vector $\{\phi\}$ and the element geometries are represented in the following form using FEM steps.

$$\{d_e\} = \sum_{i=1}^{NN} [N_i]\{d\}_i \quad , \quad \{\phi\} = \sum_{i=1}^{NN} [N_{\phi i}]\{\phi\}_i \quad , \quad x = \sum_{i=1}^{NN} [N_i]x_i \quad , \quad y = \sum_{i=1}^{NN} [N_i]y_i \tag{11}$$

where, $[N_i]$and$[N_{\phi i}]$ are the interpolation (shape function) functions for the i^{th} node, $\{d_i$ is the vector of unknown displacements for the i^{th} node and NN is the number of nodes per element. The details of the shape functions can be seen in Cook *et al*. (2009).

3.1 Governing equation

The governing equation of the nonlinear free vibration is derived using Hamilton's principle and expressed as

$$\delta \int_{t_1}^{t_2} (T - U) = 0 \tag{12}$$

Substituting Eqs. (9b) and (10) in Eq. (12) we get electromechanically coupled form of equation and can be written as

$$[M]\{\ddot{d}\} + [K_q]\{d\} + [K_{q\phi}]\{\phi\} = 0 \tag{13}$$

$$[K_{q\phi}]^T \{d\} + [K_{\phi\phi}]\{\phi\} = 0 \tag{14}$$

Now, eliminating φ from the above-mentioned equations and the modified form can be presented as

$$[M]\{\ddot{d}\} + [\overline{K}]\{d\} = 0 \tag{15}$$

where, $[\overline{K}] = [K_q] - [K_{q\phi}][K_\phi]^{-1}[K_{q\phi}]^T$

Assuming the system vibrating in principal mode with the natural frequency (ω), Eq. (15) is reduced to nonlinear generalized eigenvalue problem and the final form of the nonlinear governing equation of the laminated curved composite panel embedded with PZT can be presented as

$$\left(\left[\overline{K}\right]-\omega^2\left[M\right]\right)\left\{\overline{\phi}\right\}=0 \tag{16}$$

where, ω is the natural frequency and $\left\{\overline{\phi}\right\}$ corresponding eigenvector, respectively, for any generalized eigenvalue problem and solved using direct iterative method. The detailed steps of the solution procedure are given in a flowchart form in Fig. 2.

4. Results and discussions

In order to obtain the desired responses, a general nonlinear FE computer code has been developed in MATLAB environment using the present mathematical model considering the quadratic variation of electric potential through the thickness of laminated panel. The elastic and electrical properties of graphite/epoxy composites and PZT-5A materials are presented in Table1.

Table 1 Material properties of graphite/epoxy and PZT-5A

Elastic properties of graphite/epoxy: E_{11}=181.0GPa; E_{22}=E_{33}=10.3GPa; G_{12}=G_{13}=7.17GPa; G_{23}=0.28GPa; v_{12}=v_{13}=0.28; v_{23}=0.33; ρ=1580 kg/m3,
Elastic properties of PZT: E_{11}=E_{22}=61.0GPa; E_{33}=53.2GPa; G_{12}=22.6GPa; G_{13}=G_{23}=21.1GPa; v_{12}=0.35; v_{13}=v_{23}=0.38; ρ=7750 kg/m3,
Piezoelectric stress coefficient of PZT(C/m^2) e_{31}=e_{32}=7.209 C/m^2; e_{33}=15.118 C/m^2; e_{24}=e_{15}=12.322 C/m^2
Dielectric constant (F/m): k_{11}=k_{22}=1.53 x 10^{-8}; k_{33}=1.53 x 10^{-8}

Table 2 Support conditions

CCCC	$u_0=v_0=w_0=\theta_x=\theta_y=\theta_z=\phi_x=\phi_y=\lambda_x=\lambda_y$ at $x = 0, a$ and $y = 0, b$
SSSS	$v_0=w_0=\theta_z=\phi_y==\lambda_y=$ at $x = 0, a$; $u_0=w_0=\theta_z=\phi_x=\lambda_x=$ at $y = 0, b$
SCSC	$v_0=w_0=\theta_z=\phi_y=\lambda_y=$ at $x = 0, a$; $u_0=v_0=w_0=\theta_x=\theta_y=\theta_z=\phi_x=\phi_y=\lambda_x=\lambda_y=0$ at $y = 0, b$
HHHH	$u_0=v_0=w_0=\theta_z=\phi_y=\lambda_y=0$ at $x = 0, a$; $u_0=v_0=w_0=\theta_z=\phi_x=\lambda_x=0$ at $y = 0, b$

Table 2 presents the type of support conditions employed in the present computation to avoid rigid body motion as well as reduce the number of unknowns. The simply supported boundary has been used throughout the analysis unless specified otherwise. The nondimensional form of the fundamental frequencies is obtained using the following formulae for throughout the analysis.

$$(\varpi) = \omega b^2 \left\{ \rho / \left(E_{22} h^2 \right) \right\}^{1/2} \tag{17}$$

4.1 Convergence and comparison study

As a very first step, the convergence behaviour of the developed FE model has been checked for curved panel embedded with PZT actuators and the non-dimensional fundamental frequencies are plotted in Fig.3. The fundamental natural frequencies of cross-ply and angle-ply laminations [p/ $(90^0/0^0)_2$/p, p/ $(45^0/-45^0)_2$/p, p/ $(30^0/-30^0)_2$/p] for different support conditions with mesh refinement are plotted in the figure. Based on the convergence it is understood that, a (6×6) mesh is sufficient to compute the responses further.

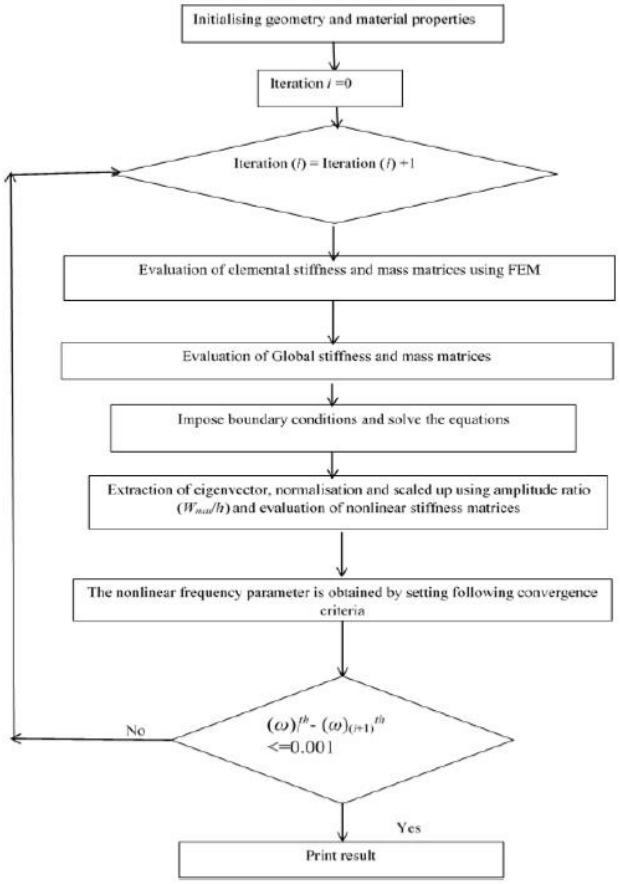

Fig. 2 Steps of solution method

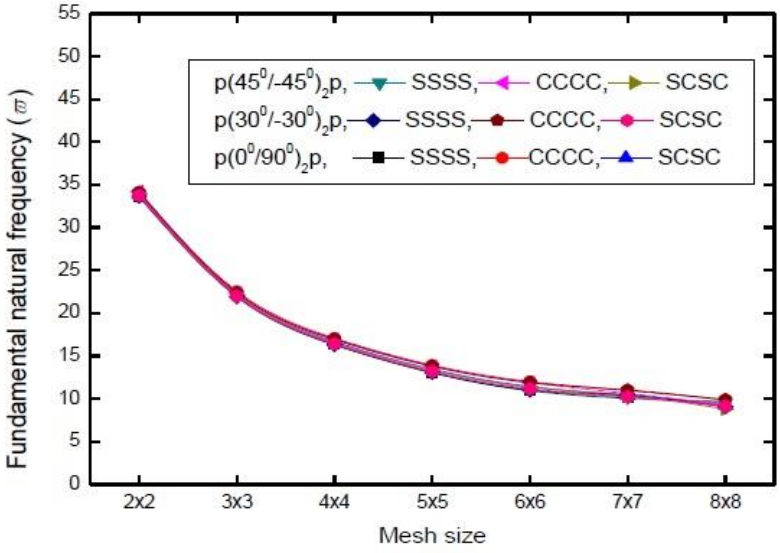

Fig. 3 Convergence behaviour of fundamental frequencies (ϖ_L) of square laminated composite spherical shell panel embedded with PZT layers for R/b=10 and b/h=20

Table 3 Comparison study of nonlinear frequency (ϖ_{NL}) of simply supported square cross-ply laminated composite shell panel embedded with PZT layers [$P/(0^0/90^0)_{2n}/P$]

Wmax/h	n	1	2	3	4
Linear (ϖ_L)	Nanda (2010)	11.6758	11.9947	12.0409	12.0564
	Present	12.0667	11.499	11.994	12.0155
0.2	Nanda (2010)	12.4803	12.8392	12.9018	12.9269
	Present	12.3448	12.0883	12.4991	12.6229
0.4	Nanda (2010)	13.4167	13.8431	13.9337	13.9734
	Present	12.9441	12.988	12.999	13.0799
0.6	Nanda (2010)	14.4313	14.961	15.0933	15.1549
	Present	13.3441	13.6991	13.7999	13.9115
0.8	Nanda (2010)	15.4856	16.1437	16.3178	16.4184
	Present	14.6879	14.8114	14.8331	15.8441
1	Nanda (2010)	16.5657	17.3744	17.6291	17.7567
	Present	15.1277	15.7334	16.2669	16.775

Table 4 Comparison study of nonlinear frequency parameter (ϖ_{NL}) of simply supported square cross-ply laminated composite spherical shell panel embedded with PZT layers $[P/(0^0/90^0)_{2n}/P]$

Wmax/h	*R*/*b*	10	20	50	100
Linear (ϖ_L)	Nanda(2010)	11.759	10.849	10.594	10.557
		10.967	10.657	10.568	10.556
0.2	Nanda(2010)	12.839	11.292	10.678	10.539
		11.216	10.774	10.589	10.493
0.4	Nanda(2010)	13.843	12.089	11.295	11.088
		11.601	11.048	10.786	10.710
0.6	Nanda(2010)	14.961	13.047	12.125	11.864
		12.051	11.3791	11.0456	10.771
0.8	Nanda(2010)	16.144	14.123	13.104	12.802
		12.536	11.787	11.390	11.279
1	Nanda(2010)	17.326	15.199	14.188	13.858
		13.083	12.285	11.418	11.651

4.2 Parametric study

Now, in this section few more examples of spherical shell panel embedded with/without PZT layers are computed for different curvature ratios (*R*/*b*), aspect ratios (*a*/*b*), thickness ratios (*b*/*h*), support conditions and lamination schemes. The effect of different parameters on the nonlinear frequency of smart shell panel are discussed in details in the following section.

4.2.1 Effect of curvature ratio on the frequency ratio

The shell geometries and their types are defined based on the curvature ratio (*R/b*) i.e., deep to shallow. The shell structures are well known for their higher stretching energy as compared to bending energy as the shell becomes deep which affect the frequency responses greatly. In order to examine the effect of curvature ratio on the nonlinear vibration behaviour of laminated composite spherical shell panel embedded with/without PZT layers the present example is solved for four curvature ratios (*R*/*b* = 10, 20, 50 and 100) and plotted in Fig.4. It is observed that there is not any appreciable change in responses after *R*/*b=50*. It is also observed that the frequency responses are suppressed due to the embedding of PZT layer at top and bottom surfaces of the parent composite shell. Moreover, spherical shell panel $[P/(0^0/90^0)_{2n}/P]$ is showing hardening type of behaviour as the amplitude ratio increases.

4.2.2 Effect of aspect ratio on the frequency ratio

The aspect ratio (*a*/*b*) is one of the most important design factor for stable configuration and

geometrical stiffness of the plate/shell structures. Hence, it is necessary to understand the effect of aspect ratio on the frequency behaviour of any structural components. The nonlinear frequency parameter of thin (b/h = 100) cross-ply spherical shallow shell panel [$P/$ $(0^0/90^0)_{2n}/P$] embedded with/without PZT layers for three different aspect ratios (a/b=0.5, 1.0 and 1.5) are examined and presented in Table 5. It is clear from the table that, the frequency parameters are increasing as the aspect ratio and the amplitude ratio increases.

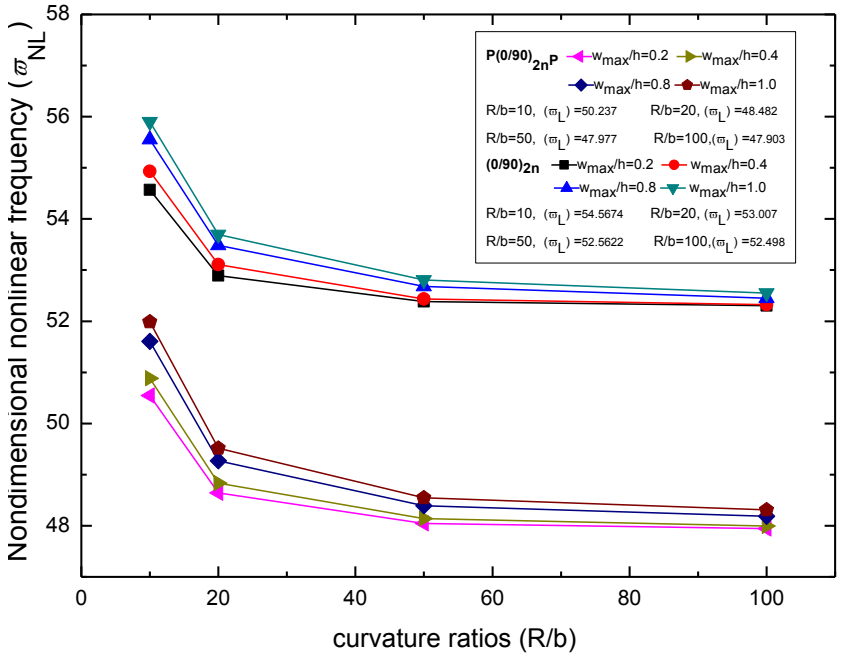

Fig. 4 Nonlinear frequency (ϖ_{NL}) of cross-ply laminated composite shell panels embedded with PZT layers [$P/(0^0/90^0)_{2n}/P$] for different curvature ratio (R/a) at b/h=20 and a/b=1

Table 5 Effect of aspect ratio (a/b) on cross-ply laminated thin composite shallow shell panel embedded with PZT layer [$P/(0^0/90^0)_{2n}/P$] (b/h = 100, R/a = 50)

a/b	Linear frequency (ϖ_L)		0.2		0.4		0.8		1.0	
	$(0/90)_2$	P$(0/90)_2$P	$(0/90)_2$	P$(0/90)_2$P	$(0/90)_2$	P$(0/90)_2$P	$(0/90)_2$	P$(0/90)_2$P	$(0/90)_2$	P$(0/90)_2$P
0.5	19.788	13.316	18.097	13.221	18.151	13.251	18.170	13.325	18.309	13.357
1.0	47.966	36.673	45.426	36.519	45.475	36.523	45.547	36.790	45.789	36.834
1.5	89.104	65.641	86.470	65.595	86.554	65.582	86.586	65.661	89.076	65.877

4.2.3 Effect of thickness ratio on the frequency ratio

Thickness ratio (b/h) plays a major role in determining the flexural behaviour of any structural component and it is more critical for laminated structures. The effect of thickness ratio on nonlinear frequency parameter of spherical shell panel bonded with/without PZT layers is computed and plotted in Fig.5. For the present case, the responses are computed for four thickness ratios (b/h = 10, 20, 50 and 100) and four amplitude ratios (W_{max}/h = 0.2, 0.4, 0.8 and 1.0). It is observed that the non-dimensional linear and nonlinear frequency parameters are increasing as the thickness ratio increases and the frequency parameters are suppressed considerably due to the embedding of the PZT layers.

4.2.4 Influence of stacking sequence and PZT layers on nonlinear frequency

In this example, the effect of stacking sequence (symmetric and anti-symmetric), number of PZT layer and PZT layer position on the nonlinear vibration behaviour of cross-ply and angle-ply laminated composite spherical shell panel is analysed and presented in Fig. 6. It can easily be observed that the PZT layers suppress the vibration frequencies substantially for both the cross-ply and angle-ply laminations. The effect of PZT layers are noticeable for cross-ply lamination as compared to the angle-ply laminations.

4.2.5 Effect of constraint condition on nonlinear vibration behaviour

Nonlinear frequency variation of square cross-ply laminated composite spherical shell panel with/without PZT layer for four different constraint conditions (CCCC, SSSS, SCSC and HHHH) are analysed in this example and shown in Table 6. It is well known that, the structural stiffness increases as the number of constraint increases and ultimately it increases the frequency parameter. The present linear frequency parameters follow the same trend i.e., highest fundamental frequency values for clamped support in comparison to all the other three cases (SSSS, SCSC and HHHH). It is also observed that the frequency responses of spherical panel are suppressed considerably due to the top and bottom PZT layer.

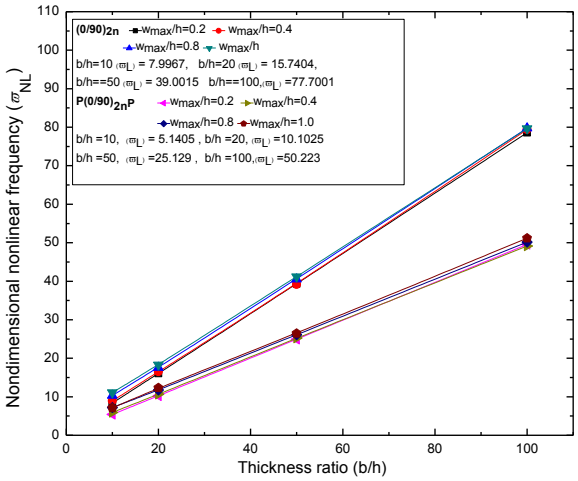

Fig. 5 Effect of thickness ratio (b/h) on frequency ratio (ϖ_{NL}/ϖ_L) of crossply laminated thin composite shallow shell panel embedded with PZT layers (R/b=10, a/b=1)

5. Conclusions

In this present article, the large amplitude free vibration behaviour of laminated composite spherical shell panels embedded with the piezoelectric layer is investigated based on the first time developed nonlinear mathematical model using the HSDT kinematics and Green-Lagrange nonlinearity. The present model also includes all the nonlinear higher order terms to count the exact flexure of the laminated composite shell panel with greater accuracy whereas the quadratic variation of electric potential across the transverse direction is considered. The governing differential equation is obtained using Hamilton's principle and discretised using nonlinear FEM steps. The desired responses are computed using direct iterative method through a homemade computer code developed in MATLAB environment. The efficacy and robustness of the present developed mathematical model have been shown by comparing the responses to that available literature. Finally, variety of numerical examples are solved for PZT embedded laminated spherical panel and the effect of different parameters on frequency parameters are discussed in detail. It is observed that the panels are showing hard spring type behaviour as the amplitude of vibration increases. It is also concluded that the curvature ratio, the thickness ratio, the aspect ratios, the support conditions and the fibre orientation have a significant effect on the nonlinear free vibration responses of laminated composite panels embedded with piezoelectric layers.

Acknowledgments

This work is under the project sanctioned by the Department of Science and Technology (DST) through grant **SERB/F/1765/2013-2014 Dated: 21/06/2013**. Authors are thankful to DST, Govt. of India for its consistent support.

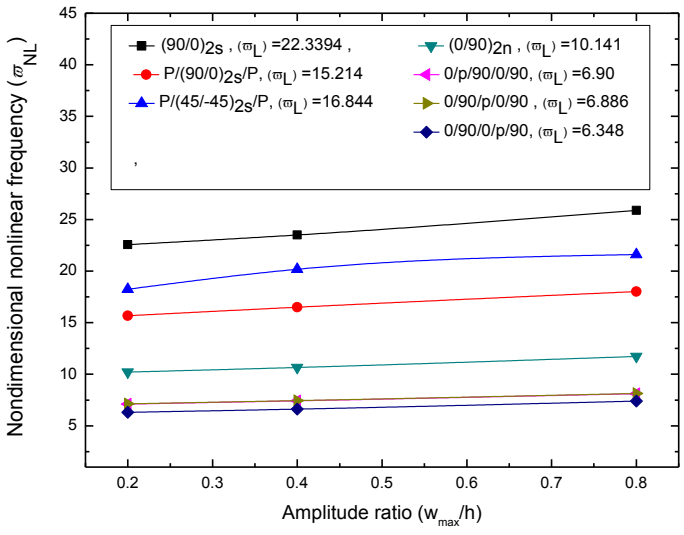

Fig. 6 Effect stacking sequence and number of PZT layers on nonlinear frequency parameter (ϖ_{NL}) of laminated composite spherical shell panels (b/h=20, a/b=1)

Table 6 Effect of support condition on nonlinear frequency parameter of spherical shell panels with/without PZT layers with b/h=30 and R/a=10

Support	Linear frequency (ϖ_L)		0.20		0.40		0.80	
Conditions	$(0/90)_2$	$P(0/90)_2P$	$(0/90)_2$	$P(0/90)_2P$	$(0/90)_2$	$P(0/90)_2P$	$(0/90)_2$	$P(0/90)_2P$
SSSS	33.333	22.405	32.259	22.958	31.610	23.565	31.610	24.971
CCCC	41.514	29.594	46.345	33.883	40.641	38.551	40.641	36.126
SCSC	39.866	28.743	39.616	31.660	43.107	34.518	43.107	34.234
HHHH	38.626	27.880	42.319	31.995	48.335	36.196	48.335	36.367

References

Arefi, M. and Khoshgoftar, M.J. (2014), "Comprehensive piezo-thermo-elastic analysis of a thick hollow spherical shell", *Smart Struct. Syst.*, **14**(2), 225-246.

Arefi, M. and Rahimi, G.H. (2011), "Nonlinear analysis of a functionally graded square plate with two smart layers as sensor and actuator under normal pressure", *Smart Struct. Syst.*, **8**(5), 433-447.

Benjeddou, A. (2000), "Advances in piezoelectric finite element modeling of adaptive structural elements: a survey", *Comput. Struct.*, **76**, 347-363.

Balamurugan, V. and Narayanan, S. (2001), "Shell finite element for smart piezoelectric composite plate/shell structures and its application to the study of active vibration control", *Finite Elem. Anal. Des.*, **37**, 713-738.

Balamurugan, V. and Narayanan, S. (2009), "Multilayer higher order piezlaminated smart composite shell finite element and its application to active vibration control", *J. Intell. Mat. Syst. Str.*, **20**, DOI: 10.1177/1045389x08095269.

Benjeddou, A. Deu, J.F. and Letombe, S. (2002), "Free vibrations of simply-supported piezoelectric adaptive plates: an exact sandwich formulation", *Thin Wall. Struct.*, **40**, 573-593.

Carrera, E., Brischetto, S. and Nali P (2011), *Plates and Shells for Smart Structures: Classical and Advanced Theories for Modeling and Analysis*, (1st Ed.), John Wiley & Sons Ltd, United Kingdom.

Cook, R.D., Malkus, D.S., Plesha, M.E. and Witt, R.J. (2009), *Concepts and applications of finite element analysis*, (4th Ed.), John Wiley & Sons, Singapore.

Chakravorty, D. Bandyopadhyay, J.N. and Sinha P.K. (1996), "Finite element free vibration analysis of doubly curved laminated composite shells", *J. Sound Vib.*, **191**(4) 491-504.

Dash, P. and Singh, B.N. (2009), "Nonlinear free vibration of piezoelectric laminated composite plate", *Finite Elem. Anal. Des.*, **45**, 686-694.

Heyliger, P. and Brooks, S. (1995), "Free vibration of piezoelectric laminates in cylindrical bending", *Int. J. Solids Struct.*, **32**(20), 2945-2960.

Huang, X.L. and Shen, H.S. (2005), "Nonlinear free and forced vibration of simply supported shear deformable laminated plates with piezoelectric actuators", *Int. J. Mech. Sci.*, **47**, 187-208.

Huang, D. and Sun, B.H. (2001), "Approximate solution on smart composite beams by using MATLAB", *Compos. Struct.*, **54**, 197-205.

Kattimani, S.C. and Ray, M.C. (2014), "Active control of large amplitude vibrations of smart magneto–electro–elastic doubly curved shells", *Int. J. Mech. Mater. Des.*, DOI: 10.1007/s10999-014-9252-3.

Kerur, S.B. and Ghosh A. (2011), "Active control of geometrically non-linear transient response of smart laminated composite plate integrated with AFC actuator and PVDF sensor", *J. Intell. Mat. Syst. Str.*, **22**, 1149-1160.

Kulkarni S.A. and Bajoria K.M. (2007), "Large deformation analysis of piezolaminated smart structures using higher-order shear deformation theory", *Smart Mater. Struct*., **16**, 1506-1516.

Lee, S.J. and Reddy, J.N. (2004), "Vibration suppression of laminated shell structures investigated using higher order shear deformation theory", *Smart Mater. Struct.*, **13,** 1176-1119.

Lee, S.J., Reddy, J.N. and Rostam-Abadi, F. (2006), "Nonlinear finite element analysis of laminated composite shells with actuating layers", *Finite Elem. Anal. Des.*, **43**, 1-21.

Nanda, N. (2010), "Non-linear free and forced vibrations of piezoelectric laminated shells in thermal environments", *The IES Journal Part A: Civil & Structural Engineering*, **3**(3), 147-160.

Rafiee, M., Mohammadi, M., Aragh, B.S. and Yaghoobi, H. (2013), "Nonlinear free and forced thermo-electro-aero-elastic vibration and dynamic response of piezoelectric functionally graded laminated composite shells Part II: Numerical results", *Compos. Struct.*, **103**, 188-196.

Ramirez, F., Heyliger, P.R. and Pan, E. (2006), "Free vibration response of two-dimensional magneto-electro-elastic laminated plates", *J. Sound Vib.*, **292**, 626-644.

Reddy, J.N. (1999), "On laminated composite plates with integrated sensors and actuators", *Eng. Struct.*, **21**, 568-593.

Reddy, J.N. (2004), "*Mechanics of laminated composite plates and shells: Theory and Analysis"*, (2nd Edition), CRC Press, Boca Raton, Florida, FL, USA.

Saravanos, D.A., Heyliger. P.R., and Hopkins, D.A. (1997), "Layerwise mechanics and finite element for the dynamic analysis of piezoelectric composite plates", *Int. J. Solids Struct.*, **34**(3), 359-378.

Sarangi, S.K. and Ray, M.C. (2011), "Active damping of geometrically nonlinear vibrations of doubly curved laminated composite shells", *Compos. Struct.*, **93**, 3216-3228.

Sarangi, S.K. and Ray, M.C. (2010), "Smart damping of geometrically nonlinear vibrations of laminated composite beams using vertically reinforced 1–3 piezoelectric composites", *Smart Mater. Struct.*, **19**(075020), 1-14.

Singh, V.K. and Panda S.K. (2014), "Nonlinear free vibration analysis of single/doubly curved composite shallow shell panels", *Thin Wall. Struct.*, **85**, 341-349.

Xu, K., Noor, A.K. and Tang, Y.Y. (1997), "Three-dimensional solutions for free vibrations of initially-stressed thermoelectroelastic multilayered plates", *Comput. Method. Appl. M.*, **141**, 125-139.

BS

Appendix A

The individual terms of operator and thickness coordinate matrices:

$$\left[B_{\phi}\right]=\begin{bmatrix} -\partial/\partial x & -\partial/\partial y & 0 & 0 & 0 & 0 & 0 & 0 \\ 0 & 0 & -\partial/\partial x & -\partial/\partial y & 0 & 0 & -1 & 0 \\ 0 & 0 & 0 & 0 & -\partial/\partial x & -\partial/\partial y & 0 & -2 \end{bmatrix}^{T}$$

$$\left[T_{\phi}\right]=\begin{bmatrix} 1 & 0 & z & 0 & z^2 & 0 & 0 & 0 \\ 0 & 1 & 0 & z & 0 & z^2 & 0 & 0 \\ 0 & 0 & 0 & 0 & 0 & 0 & 1 & 1 \end{bmatrix} \quad \text{and} \quad \{d\}=\{u_0, v_0, w_0, \theta_x, \theta_y, \theta_z, \phi_x, \phi_y, \lambda_x, \lambda_x\}$$

Nomenclature

(X,Y,Z)	Cartesian coordinate axes
(u,v,w)	Displacements along X,Y and Z directions
(u_0,v_0,w_0)	The displacements of a point on the mid-plane of the panel along X,Y and Z direction
R_x, R_y	Principal radii of curvature of shell panel along the corresponding material line
a, b, h	Length , breadth and thickness of panel
θ_x , θ_y	Rotations along y and x direction respectively
θ_z , ϕ_x, ϕ_y , λ_x , λ_y	Higher order terms of Taylor series expansion
ε_L , ε_{NL}	Linear and nonlinear strain vector
$\{d\}$	Global displacement vector
E	Electric field intensity
G	Shear modulus
v	Poisson's ratio
$[K]$,$[KN_1]$,$[KN_2]$	Linear and nonlinear stiffness matrices
$[K_q]$, $[K_{q\phi}]$, $[K_{\phi\phi}]$	echanical, coupled electro-mechanical and electrical stiffness matrices respectively
$[T]$, $[f]$	Function of thickness coordinate
U	Total strain energy
V	Total kinetic energy
$W_{\max}$	Maximum central deflection of the shell panel
$W_{\max}/h$	Amplitude ratio
ϖ_L and ϖ_{NL}	Non-dimensional linear and nonlinear frequencies
ϖ_{NL}/ϖ_L	Frequency ratio, nonlinear frequency to linear frequency
ϕ	Electric potential
$\left[B_\phi\right]$	Electric Differential operator matrix

$[T_\phi]$ Electric thickness coordinate matrix